Part I
Basic Aspects and Extension of Methods

Handbook of Chaos Control, 2nd Ed. Edited by E. Schöll and H.G. Schuster

ISBN: 978-3-527-40605-0

1
Controlling Chaos

Elbert E. N. Macau and Celso Grebogi

1.1
Introduction

The concept of "control" is associated with the idea of implementing actions to guarantee that a system behaves as desired. Nature is prodigal in presenting sophisticated control strategies that regulated phenomena that take place in all scales of time and space [13, 18, 35, 49]. These mechanisms reach the ultimate level of efficacy and refinement on biological systems in which they are responsible for the emergence of the sustainable phenomenon of life. A careful and systematic investigation performed on mechanisms Nature uses for system control uncover that they are based on the following concepts: stability, feedback, and flexibility.

Stability can be defined as the system's ability for keeping itself working properly even when perturbations act on it. This is the main goal to be achieved by the control strategy that is embedded in the system. Every system is supposed to operate properly inside well-defined regions. During its lifetime operation, a system suffers all kinds of internal and external perturbations. In order to continue its appropriate operation, a system must be stable enough to those perturbations. This ability can be seen around us in natural processes and is closely related to the concept of feedback [18, 49], which can be defined as the mechanism whereby part of the system output is returned (back) to be used as input of the control strategy, providing self-regulation. Through this mechanism, a system regulates itself by monitoring its own output to keep it stable and operating properly. To accomplish that, control strategies presented in Nature exploit another key property of the Nature: flexibility. The idea behind this concept is that it is not necessary to stress the system and drive it brutally to the desired operation point immediately or directly. In contrast, it is more efficient, reliable, and realizable to control the system by letting it to fluctuate and eventually change its dynamics as little as possible to drive it to the desired state without applying intense forces. An excess of control may result in energy waste and eventually could imply in system damage. Thus, the concepts of stability, feed-

Handbook of Chaos Control, 2nd Ed. Edited by E. Schöll and H. G. Schuster

ISBN: 978-3-527-40605-0

back and flexibility are wisely combined and exploited by Nature through control strategies that allow it to opportunistically accomplish its process with remarkable efficiency.

Let us now explore how this scenario, inspired from Nature, fits on the concept of chaos control [21, 22, 33, 39]. At first, it is necessary to properly understand the meaning of chaotic dynamics [2, 14]. The sensitive dependence on initial condition is the main characteristic of chaotic behavior. It means that two trajectories that are initialized very close to each other separate exponentially in time. Because of this typical behavior, which is known as the "butterfly effect," long time prediction of a chaotic trajectory based on finite precision measurements is impossible. However, this characteristic also implies that a chaotic trajectory is extremely sensitive to the effect of perturbations. As so, just a small perturbation applied at a given time is enough to change the trajectory's future evolution, directing its way to other regions of the chaotic invariant set [25]. Another key characteristic of the chaotic system is that there are an infinite variety of behaviors embedded on it. A chaotic system contains a dense orbit on the invariant set, which is a chaotic trajectory that recurrently passes infinitely close to any point of that set. A third characteristic is that the chaotic invariant set contains an infinite number of unstable periodic orbits of all periods, which coexist with the chaotic motion. These orbits are unstable in the sense that small deviation from the periodic orbit grows exponentially rapidly in time, and the system quickly moves away from the periodic orbit in a chaotic trajectory. The combination of these three characteristics makes chaotic systems as one of the most flexible systems that can be found in Nature. It is exactly these characteristics that are explored in the scenario of chaos control.

Chaos control is based on the idea of exploiting the key dynamical characteristics just presented to control the system as desired [21, 22, 33, 39]. As so, the sensitive dependence on the initial condition is used both to stabilize chaotic behavior in periodic orbits [21, 22, 33, 39] and to direct trajectories to a desired state [30, 34, 44–46]. Small perturbations applied to control parameters can be used to stabilize chaos, keeping the parameters in the neighborhood of their nominal values. This idea that came about in the context of the OGY method of control of chaos [39] and its feasibility has been experimentally demonstrated in several experiments [1, 4, 5, 8, 15, 17, 26, 37, 41]. Besides, a carefully chosen sequence of small perturbations applied to some control parameter can also be used to rapidly direct trajectories to some desired final state [44–46]. This strategy of guiding trajectories in chaotic systems, called targeting, also had its feasibility experimentally demonstrated [7]. On both these approaches we can verify how the fundamental idea of the chaos control is applicable: the system flexibility is paramount and opportunistically exploited so that the perturbations do not significantly change the system dynamics, but just enable the intrinsic system dynamics to accomplish the desired control task. In some sense, the control of chaos mimics the way that Nature implements its control strategy to opportunistically accomplish its goals. Furthermore, to extremely exploit the flexibility presented on chaotic systems, the controller that implements the chaos control

strategy must preserve the chaotic dynamics at all time. As so, the feedback concept, when used, is applied just locally, in the neighborhood of a specific chaotic trajectory, and implemented so that just small perturbations are applied on the chaotic trajectory with the goal of keeping the whole system stable and operating properly.

Over the years, the concept of control of chaos has been successfully applied on a variety of systems and on a multitude of circumstances. However, the horizon of applicability is still wider. In a typical application, we see a control of chaos strategy applied in a situation in which the chaotic dynamics develops on a chaotic attractor. However, chaotic dynamics are present not only on chaotic attractors [25, 48], but also on nonattracting chaotic sets, giving rise to important phenomena with remarkable physical consequences for the dynamical system in which they are present. These are the cases of chaotic transients [24, 28], chaotic scattering [9, 27], and fractal basing boundaries [20, 23]. In these phenomena, a typical trajectory presents over time different behaviors in which a chaotic behavior is followed by a nonchaotic one. The dynamics is understood by the presence of chaotic saddles. A chaotic saddle is an invariant chaotic set that can be envisioned as the intersection of its stable and unstable manifolds, where the stable and unstable manifolds each consist of a Cantor set of surfaces. As so, it is a fractal object and it has chaotic trajectories that never leave the set. It can be understood by the horseshoe model, introduced by Smale [48], who, by using symbolic dynamics, showed that this invariant set has a dense orbit, exhibits the sensitivity to initial condition property, and embedded in it there is a countable infinity set of unstable periodic orbits of arbitrary high periods. Let us consider a system in which a nonattracting chaotic saddle Γ coexists in the phase space with others nonchaotic attractors. As there are other attractors in the phase space, all initial conditions, except for a set of measure zero made up of the chaotic saddle Γ and its stable manifold, generate trajectories that asymptote to one of the attractors. Trajectories starting from random initial conditions may wander near the chaotic saddle Γ for a finite time before settling down into one of the attractors. During the time interval in which a trajectory suffers the influence of the chaotic saddle, it behaves as a chaotic trajectory. Furthermore, the closer the initial condition of a trajectory to the stable manifold of Γ, longer the trajectory stays near the chaotic saddle, exhibiting a chaotic-like behavior.

If we have a chaotic system whose dynamics is governed by a chaotic saddle, control of chaos strategy can be combined with classic control methods to give rise to a powerful control approach that exploits the flexibility that the combined methods can offer. It can be accomplished as follows: for an ordinary trajectory, whenever it behaves as a chaotic one, a control of chaos strategy is applied. As soon as the trajectory leaves the region of the phase space in which it behaves as a chaotic one, control of chaos is switched off and a classic control mechanism starts to be in effect. With this approach that we could call as *opportunistic chaos control*, we have the most effective control approach in action for each of the conceivable dynamical behaviors that a system may present. In fact, this hy-

pothetical situation is very common in Nature and in technological systems. In this chapter, we present some key examples that show the efficiency of this approach. Therefore, we proceed as follows. In the next two sections, we review the OGY method of chaos control as it was originally proposed and our targeting strategy that can be applied even to higher dimensional systems. After that, we show an application example where a classic control method is used in association with the OGY to properly control an electronic system. In the subsequent section, our targeting method is associated with the classic control method to efficiently control a system with a very elaborated dynamics. Finally, we end this chapter with remarks about the concept of control of chaos.

1.2 The OGY Chaos Control

The key ingredient for the control of chaos [38, 39] is the observation that a chaotic invariant set has embedded on it an infinite and enumerable set of unstable periodic orbits of all periods. Counting on ergodicity [25], another intrinsic property of the chaotic behavior, we wait for a natural passage of the chaotic trajectory close to the desired periodic behavior and then a small judiciously chosen controlling perturbation is applied. This small perturbation is enough to stabilize the system in the desired periodic behavior. Through this mechanism, the system can operate on a large number of different set points (theoretically, an infinite number of them), with a great flexibility in switching among them.

In this section, we review the main points related to the originally proposed algorithm. As so, our scenario is a chaotic dynamical system whose attractor is a three-dimensional state space. A Poincaré section [2] can be introduced transversal to the chaotic flow so that the system dynamics on this Poincaré section can be described by a two-dimensional invertible map as

$$\boldsymbol{x}_{\mathbf{n}+1} = \mathbf{F}(\boldsymbol{x}_{\mathbf{n}}, p), \tag{1.1}$$

where $\boldsymbol{x}_{\mathbf{n}} \in \boldsymbol{R}^2$, $\mathbf{F}$ is a smooth function of its variables, and $p \in \boldsymbol{R}$ is an externally accessible control parameter. Following the idea of using small perturbations to control the system, parameter allowed variations must be small,

$$|p - \bar{p}| < \delta, \tag{1.2}$$

where $\bar{p}$ is the nominal parameter value, and $\delta \ll 1$ defines the allowable range of parameter variation. We wish to program the parameter p so that a chaotic trajectory is stabilized when it enters in a neighborhood of the target periodic orbit.

Let $\boldsymbol{x}_{\mathbf{F}}(\bar{p})$ be one of the fixed points of the map (1.1) at the nominal parameter value $\bar{p}$ that we wish to stabilize. (The extension of the method for unstable periodic points of period larger than 1 is straightforward.) The location of the fixed

point in the phase space depends on the control parameter p. Upon application of small perturbation Δp, we have $p = \bar{p} + \Delta p$. Since Δp is small, we expect $\boldsymbol{x}_{\mathbf{F}}(p)$ to be close to $\boldsymbol{x}_{\mathbf{F}}(\bar{p})$. We write

$$\boldsymbol{x}_{\mathbf{F}}(p) \approx \boldsymbol{x}_{\mathbf{F}}(\bar{p}) + \boldsymbol{g}\Delta p, \tag{1.3}$$

where the vector $\boldsymbol{g}$ is given by

$$\boldsymbol{g} \equiv \frac{\partial \boldsymbol{x}_{\mathbf{F}}}{\partial p}|_{p=\bar{p}} \approx \frac{\boldsymbol{x}_{\mathbf{F}}(p) - \boldsymbol{x}_{\mathbf{F}}(\bar{p})}{\Delta p}. \tag{1.4}$$

The system dynamics of any smooth nonlinear system is approximately linear in a small ε-neighborhood of a fixed point. Thus, near $\boldsymbol{x}_{\mathbf{F}}(\bar{p})$, we can use the linear approximation for the map:

$$[\boldsymbol{x}_{\mathbf{n+1}} - \boldsymbol{x}_{\mathbf{F}}(p)] \approx \boldsymbol{M}[\boldsymbol{x}_{\mathbf{F}}(p)] \cdot [\boldsymbol{x}_{\mathbf{n}} - \boldsymbol{x}_{\mathbf{F}}(p)], \tag{1.5}$$

where $\boldsymbol{M}[\boldsymbol{x}_{\mathbf{F}}(p)]$ is the 2×2 Jacobian matrix of the map $\mathbf{F}(\boldsymbol{x}, p)$ evaluated at the fixed point $\boldsymbol{x}_{\mathbf{F}}(p)$, which is defined as follows:

$$\boldsymbol{M}[\boldsymbol{x}_{\mathbf{F}}(p)] = \frac{\partial \mathbf{F}}{\partial \boldsymbol{x}}|_{\boldsymbol{x}_{\mathbf{F}}(p)} \approx \boldsymbol{M}[\boldsymbol{x}_{\mathbf{F}}(\bar{p})] + \frac{\partial \boldsymbol{M}}{\partial p}|_{p=\bar{p}}\Delta p. \tag{1.6}$$

Note that $\Delta p \sim \varepsilon$ and $||[\boldsymbol{x}_{\mathbf{n}} - \boldsymbol{x}_{\mathbf{F}}(p)]|| \sim \varepsilon$, where ε is the size of the small neighborhood in which the linear approximation (1.5) is valid. Writing $\boldsymbol{x}_{\mathbf{F}}(p) \approx \boldsymbol{x}_{\mathbf{F}}(\bar{p}) + \boldsymbol{g}\Delta p$ (from Eq. (1.4)), substituting this relation and Eq. (1.6) into Eq. (1.5), and keeping only terms which are first order in ε, we obtain

$$\boldsymbol{x}_{\mathbf{n+1}} - \boldsymbol{x}_{\mathbf{F}}(\bar{p}) \approx \boldsymbol{g}\Delta p + \boldsymbol{M}[\boldsymbol{x}_{\mathbf{F}}(\bar{p})] \cdot [\boldsymbol{x}_{\mathbf{n}} - \boldsymbol{x}_{\mathbf{F}}(\bar{p}) - \boldsymbol{g}\Delta p]. \tag{1.7}$$

In Eq. (1.7), the Jacobian matrix $\boldsymbol{M}$ is evaluated at the fixed point $\boldsymbol{x}_{\mathbf{F}}(\bar{p})$ of the unperturbed system, which is the one to be stabilized. Since $\boldsymbol{x}_{\mathbf{F}}(\bar{p})$ is embedded in the chaotic attractor, it is unstable and it has one stable and one unstable direction [4]. Let $\boldsymbol{e}_{\mathbf{s}}$ and $\boldsymbol{e}_{\mathbf{u}}$ be the stable and unstable unit eigenvectors at $\boldsymbol{x}_{\mathbf{F}}(\bar{p})$, respectively, and let $\boldsymbol{f}_{\mathbf{s}}$ and $\boldsymbol{f}_{\mathbf{u}}$ be two unit vectors that satisfy $\boldsymbol{f}_{\mathbf{s}} \cdot \boldsymbol{e}_{\mathbf{s}} = \boldsymbol{f}_{\mathbf{u}} \cdot \boldsymbol{e}_{\mathbf{u}} = 1$ and $\boldsymbol{f}_{\mathbf{s}} \cdot \boldsymbol{e}_{\mathbf{u}} = \boldsymbol{f}_{\mathbf{u}} \cdot \boldsymbol{e}_{\mathbf{s}} = 0$, which are the relations by which the vectors $\boldsymbol{f}_{\mathbf{s}}$ and $\boldsymbol{f}_{\mathbf{u}}$ can be determined from the eigenvectors $\boldsymbol{e}_{\mathbf{s}}$ and $\boldsymbol{e}_{\mathbf{u}}$. The vectors $\boldsymbol{f}_{\mathbf{s}}$ and $\boldsymbol{f}_{\mathbf{u}}$ are contravariant basis vectors associated with the eigenspace $\boldsymbol{e}_{\mathbf{s}}$ and $\boldsymbol{e}_{\mathbf{u}}$. The Jacobian matrix $\boldsymbol{M}[\boldsymbol{x}_{\mathbf{F}}(\bar{p})]$ can then be written as:

$$\boldsymbol{M}[\boldsymbol{x}_{\mathbf{F}}(\bar{p})] = \lambda_u \boldsymbol{e}_{\mathbf{u}}\boldsymbol{f}_{\mathbf{u}} + \lambda_s \boldsymbol{e}_{\mathbf{s}}\boldsymbol{f}_{\mathbf{s}}, \tag{1.8}$$

where λ_s and λ_u are the stable and unstable eigenvalues in the eigendirections $\boldsymbol{e}_{\mathbf{s}}$ and $\boldsymbol{e}_{\mathbf{u}}$, respectively.

When the trajectory point $\boldsymbol{x}_{\mathbf{n}}$ falls into small ε-neighborhood of the desired fixed point $\boldsymbol{x}_{\mathbf{F}}(\bar{p})$ so that Eq. (1.5) applies, a small parameter perturbation Δp_n is

applied at time n to make the fixed point shift slightly so that at the next iteration $(n+1)$, $\boldsymbol{x}_{\mathbf{n+1}}$ falls on the stable direction of $\boldsymbol{x}_{\mathbf{F}}(\bar{p})$. Thus, we choose the parameter control Δp_n such that

$$\boldsymbol{f}_{\mathbf{u}} \cdot [\boldsymbol{x}_{\mathbf{n+1}} - \boldsymbol{x}_{\mathbf{F}}(\bar{p})] = 0. \tag{1.9}$$

If $\boldsymbol{x}_{\mathbf{n+1}}$ falls on the stable direction of $\boldsymbol{x}_{\mathbf{F}}(\bar{p})$, we can then set the control perturbation to zero, and the trajectory for subsequent time will approach the fixed point at the geometrical rate λ_s. Thus for sufficiently small $[\boldsymbol{x}_{\mathbf{n}} - \boldsymbol{x}_{\mathbf{F}}(\bar{p})]$, we can substitute Eq. (1.7) into Eq. (1.9) to obtain $\Delta p_n = c_n$:

$$c_n = \frac{\lambda_u \boldsymbol{f}_{\mathbf{u}} \cdot [\boldsymbol{x}_{\mathbf{n}} - \boldsymbol{x}_{\mathbf{F}}(\bar{p})]}{(\lambda_u - 1)\boldsymbol{f}_{\mathbf{u}}\boldsymbol{g}} \equiv \boldsymbol{C}[\boldsymbol{x}_{\mathbf{n}} - \boldsymbol{x}_{\mathbf{F}}(\bar{p})]. \tag{1.10}$$

We assume in the above that the generic condition $\boldsymbol{g} \cdot \boldsymbol{f}_{\mathbf{u}} \neq 0$ is satisfied so that $c_n \sim |\boldsymbol{x}_{\mathbf{n}} - \boldsymbol{x}_{\mathbf{F}}(\bar{p})|$, which is small. The considerations above apply only to a local small neighborhood of $\boldsymbol{x}_{\mathbf{F}}(\bar{p})$. Globally, we can specify the parameter perturbation Δp_n by setting $\Delta p_n = 0$ if $|c_n|$ is too large, since the range of the parameter perturbation is limited by Eq. (1.2). Thus, practically, we can take Δp_n to be given by

$$\Delta p_n = \begin{cases} c_n & \text{if } |c_n| < \delta \\ 0 & \text{if } |c_n| \geq \delta, \end{cases} \tag{1.11}$$

where in the definition of c_n in Eq. (1.10), it is not necessary to restrict the quantity $|\boldsymbol{x}_{\mathbf{n}} - \boldsymbol{x}_{\mathbf{F}}(\bar{p})|$ to be small.

This method can be extended to higher dimensional systems.

1.3 Targeting–Steering Chaotic Trajectories

The inherent exponential sensitivity of chaotic time evolution to perturbations can be intelligently exploited to direct the dynamics of the system to some desired state using a carefully chosen sequence of small perturbations to some system parameter. This approach, which is of fundamental interest for the control system, is called *targeting* [45].

The targeting idea came about as a way to get around an excessive transient time associated with the use of the OGY method of chaos control to higher dimensional systems. As we saw in the previous section, this method relies on the topological transitivity of the system on the invariant set Λ to bring a chaotic orbit close enough to a neighborhood of the periodic orbit on which we want to stabilize the system. This procedure works. Nevertheless, it presents a significant problem: the *transport time* can be excessively long. Besides, this time depends sensitively on the initial conditions and on the system's dimension. In

dissipative chaotic systems, for randomly chosen initial conditions, the *average transport time* is typically ε^{-D}, where ε is the linear dimension of the neighborhood about the periodic orbit, and D is the pointwise dimension at the periodic point [29]. For low values of D, this time can be acceptably small. However, for systems of higher dimension, it may have a prohibitively large value.

Let us consider a discrete time dynamical system,

$$\mathbf{X}_{i+1} = \mathbf{F}(\mathbf{X}_i, p), \tag{1.12}$$

where $\mathbf{X}_i \in \Re^n$, $p \in \Re$ is an externally controllable parameter that can be externally modified, and $\mathbf{F}$ is a smooth function in both variables. The nominal value of the parameter is $p = \bar{p}$, for which $\mathbf{F}$ is chaotic on a compact, invariant set $\Lambda \subset \Re^n$. Suppose we have two points $\mathbf{X}_s$ and $\mathbf{X}_t$ in Λ. Consider $B_\varepsilon(\mathbf{X}_s)$ a ball of radius ε around $\mathbf{X}_s$, and another ball $B_\varepsilon(\mathbf{X}_t)$ of radius ε about $\mathbf{X}_t$. The *targeting goal* is to find a *constructive orbit* that goes from a point $\mathbf{p}_{\mathbf{X}_s} \in B_\varepsilon(\mathbf{X}_s)$ to a point $\mathbf{p}_{\mathbf{X}_t} \in B_\varepsilon(\mathbf{X}_t)$. Through that constructive orbit, the inherent exponential sensitivity of a chaotic time evolution to perturbations is intelligently exploited to direct trajectories to a desired state in the shortest possible time, by the use of a carefully chosen sequence of small perturbation to some control parameter. Furthermore, since these perturbations are sufficiently small, they do not significantly change the system's dynamics, but enable the intrinsic system dynamics to drive the trajectory to the desired state.

Our technique is subdivided into two sequential parts [34]. In the first one, we find the previously described points $\mathbf{p}_{\mathbf{X}_s}$ and $\mathbf{p}_{\mathbf{X}_t}$ so that there is an orbit (real) that goes from $\mathbf{p}_{\mathbf{X}_s}$ to $\mathbf{p}_{\mathbf{X}_t}$.

In the second part, this orbit is used to build a constructive orbit (virtual) that allows the transport from $\mathbf{p}_{\mathbf{X}_s}$ to $\mathbf{p}_{\mathbf{X}_t}$ using smaller number of elements, i.e., of real orbits. In this process, small perturbations to the control parameter are used to move among the real orbits. The effect of these perturbations is to change the system's evolution from one real orbit to another, resulting in a constructive orbit that allows the transfer from $\mathbf{p}_{X_s}$ to $\mathbf{p}_{X_t}$ in a faster time. Thus, the overall effect of this procedure is to produce a suboptimal solution that is gotten by the elimination of parts of the orbit where *recurrences* occur with the use of small perturbations.

1.3.1 Part I: Finding a Proper Trajectory

The main idea of the first part of our technique is as follows [45, 46]: consider a line segment $\overline{a_1 b_1} \subset B_\varepsilon(\mathbf{X}_s)$, so that $\mathbf{X}_s$ is its middle point. To find $\mathbf{p}_{\mathbf{X}_s}$, $\overline{a_1 b_1}$ is iterated in the forward direction, while the region $B_\varepsilon(x_t)$ is iterated in the backward direction, until the forward iterated segment intersect the backward iterated region at the point $\mathbf{p}_I$. It is important to say that it is again the transitivity of a chaotic system that assures that $\mathbf{p}_I$ will be found. When the intersection is found, there is a trajectory that goes from $\mathbf{p}_{\mathbf{X}_s} \in \overline{a_1 b_1}$ to $B_\varepsilon(\mathbf{X}_t)$ through the in-

tersection $\mathbf{p}_I$. Note that $\mathbf{p}_{\mathbf{X}_s}$ can be found by iterating $\mathbf{F}$ in the backward direction from $\mathbf{p}_I$. The point $\mathbf{p}_{\mathbf{X}_s}$ is then used to determine the value $\widetilde{p}$ of the parameter that must be applied to the system to bring it from $\mathbf{X}_s$ to $\mathbf{p}_{\mathbf{X}_s}$. The following algorithm describes how that technique can be implemented:

Step 1: Define a direction Θ in space and using this direction construct a line segment $\overline{a_1 b_1} \subset B_\varepsilon(\mathbf{X}_s)$, so that $\mathbf{X}_s$ is its middle point. Call a_1 as c_0, and b_1 as c_{n_p}.

Step 2: Generate N random points $\{d_j\}_{j=1}^{N}$ inside $B_\varepsilon(\mathbf{X}_t)$.

Step 3: Create a partition of n_p subsets in $\overline{c_0 c_{n_p}}$ using a sequence of $n_p - 1$ interior points $\{c_j\}_{j=1}^{n_p-1}$.

Step 4: Using $\{d_j\}_{j=1}^{N}$, construct a Delaunay triangulation (Watson 1981; Varosi et al. 1987) T, which has the sequence of cells $\{F_j\}_{j=1}^{M}$.

Step 5: Iterate in the forward direction $\{c_j\}_{j=1}^{n_p-1}$ and use linear interpolation to approximate the resultant curve delimited by each pair of iterated points.

Step 6: Iterate in the backward direction $\{d_j\}_{j=1}^{N}$ and use linear interpolation to approximate the iterated cells of the Delaunay triangulation T.

Step 7: Continue the iteration described in steps 5 and 6 until finding the intersection $\mathbf{p}_I$ between $\overline{\mathbf{F}^l(c_k)\mathbf{F}^l(c_{k+1})}$ and $\mathbf{F}^{-l}(F_h)$, where this one is the backward iterated cell found by linear interpolation of the backward iteration of the points that delineate the cell F_h.

Step 8: Consider the middle point c_{md} of the segment $\overline{c_k c_{k+1}}$. Identify if the intersecting segment is $\overline{c_k c_{\mathrm{md}}}$ or $\overline{c_{\mathrm{md}} c_{k+1}}$. In the first case, assign the value of c_{md} to c_{k+1}; otherwise, assign the value of c_{md} to c_k. Applying a similar procedure, find a new cell F_h which is smaller than the previous one, but still contains in its face p_{x_t}.

Step 9: If $d[c_k, c_{k+1}] > \delta_l$, where δ_l is a specified limit on the precision, then repeat step 8. Otherwise, $\mathbf{p}_{\mathbf{X}_s}$ is equal to c_k.

Step 10: Using $\mathbf{p}_{\mathbf{X}_s}$, determine the value of $\widetilde{p}$ that drives the system from $\mathbf{X}_s$ to $\mathbf{p}_{\mathbf{X}_s}$. When the system gets $\mathbf{p}_{\mathbf{X}_s}$, return the parameter to its nominal value, i.e., $\overline{p}$. From there, the system dynamics will conduct the system evolution to a point $\mathbf{p}_{\mathbf{X}_t} \in B_\varepsilon(x_t)$ in $2 * l$ iterates.

With the use of this procedure, the average transport time to go from the source point to the target point typically scales logarithmically with the inverse of the size of the target region [45], which contrasts with the exponential increasing that takes place if this algorithm is not used.

1.3.2
Part II: Finding a Pseudo-Orbit Trajectory

Part I of our method produces an orbit that goes from $\mathbf{p}_{\mathbf{X}_s}$ to $\mathbf{p}_{\mathbf{X}_t}$. Let us represent that orbit by the following sequence of points $\{\mathbf{X}_i\}_{i=0}^{N}$ in $\Re^n$, where $\mathbf{X}_0 = \mathbf{p}_{x_s}$, and $\mathbf{X}_N = \mathbf{p}_{\mathbf{X}_t}$. As that orbit belongs to a chaotic trajectory in a compact invariant set Λ, it might have recurrent points [10, 11, 32, 34]. In Part II,

we look for those *recurrent points* by using a sequential search [31]. If $\mathbf{X}_r$ is a recurrent point, it means that it belongs to a sequence of points $\{\ldots, \mathbf{X}_r, \mathbf{X}_{r+1}, \ldots, \mathbf{X}_{r+n}, \ldots\}$ such that $d[\mathbf{X}_r, \mathbf{X}_{r+n}] < \delta$, making up a kind of *loop*. If none of the points inside the loop is located in $B_\varepsilon(\mathbf{X}_t)$, that loop does not effectively conduct the trajectory to the targeting point. Thus, after being identified, our method replaces that loop by a smaller orbit that is backward asymptotic to $\mathbf{X}_r$ and forward asymptotic to $\mathbf{X}_{r+n}$ [6, 29]. By creating patches like that to the recurrent points of the original orbit, we build a *constructive orbit* or a *pseudo-orbit* that allows the transportation from $\mathbf{p}_{\mathbf{X}_s}$ to $\mathbf{p}_{\mathbf{X}_t}$ with considerably less iterations than the original orbit. However, to accomplish that, perturbations must be introduced in order to switch the trajectory along the pseudo-orbits, as described next [10, 11, 32, 34].

In a hyperbolic situation, it is known that if the distance between $\mathbf{X}_r$ and $\mathbf{X}_{r+n}$ is sufficiently small, say less than δ_{lim}, then the unstable manifold of $\mathbf{X}_r$, $W^u_\varepsilon(\mathbf{X}_r)$ and the stable manifold or $\mathbf{X}_{r+n}$, $W^s_\varepsilon(\mathbf{X}_{r+n})$ intersect each other in a point $\mathbf{q}$. This fact can be exploited to accomplish our goal if a proper perturbation is applied to the sequence of points of the original orbit that passes through $\mathbf{X}_r$. In fact, according to the theorem of Hirsh and Pugh (Arrowsmith 1994), $\mathbf{q} \in W^u_\varepsilon(\mathbf{X}_r) \cap W^s_\varepsilon(\mathbf{X}_{r+n})$ implies that forward iterations of $\mathbf{q}$ converge to forward iterations of $\mathbf{X}_{r+n}$, i.e., $\lim_{k\to\infty} d[\mathbf{F}^k(\mathbf{q}), \mathbf{F}^k(\mathbf{X}_{r+n})] = 0$, and backward iterations of q converges to backward iterations of $\mathbf{X}_r$, i.e., $\lim_{k\to\infty} d[\mathbf{F}^{-k}(\mathbf{q}), \mathbf{F}^{-k}(\mathbf{X}_r)] = 0$. Thus, if we consider a point $\mathbf{X}_{r-m}$ that precedes $\mathbf{X}_r$ in the original trajectory, and a point $\mathbf{X}_{r+n+t}$ that succeeds $\mathbf{X}_{r+n}$ in the original trajectory, we have $d[\mathbf{F}^t(\mathbf{q}), \mathbf{F}^t(\mathbf{X}_{r+n})] = \varepsilon_{r+n+t}$, and $d[\mathbf{F}^{-m}(\mathbf{q}), \mathbf{F}^{-m}(\mathbf{X}_r)] = \varepsilon_{r-m}$. Furthermore, as $W^u_\varepsilon(\mathbf{X}_r)$ can be locally approximated by $E^u_{\mathbf{X}_r}$, which is the unstable subspace of the tangent space at $\mathbf{X}_r$, while $W^s_\varepsilon(\mathbf{X}_{r+n})$ can be locally approximated by $E^s_{x_{r+n}}$, which is the stable subspace of the tangent space at $\mathbf{X}_{r+n}$, and that approximation is continuously preserved over the iterations by the Jacobian of $\mathbf{F}$, i.e., $D\mathbf{F}(\cdot)$ calculated at the iteration point [25]. It follows that ε_{r-m} is located in the direction of $E^u_{\mathbf{X}_{r-m}}$, and ε_{r+n+t} is located in the direction of $E^s_{\mathbf{X}_{r+n+t}}$. Thus, if the proper perturbation ε_{r-m} is applied in the direction of $E^u_{\mathbf{X}_{r-m}}$, it produces a perturbed orbit that passes through $\mathbf{q}$, and converges to the original trajectory after $\mathbf{X}_{r+n}$. Consequently, that procedure generates the desired patch that avoids the recurrent loop of the original trajectory. In addition, that argument indicates that the perturbation ε_{r-m} can be calculated by solving the following equation:

$$\mathbf{F}^{m+t}(\mathbf{X}_{r-m} + \varepsilon_{r-m} E^u_{\mathbf{X}_{r-m}}, \overline{p}) = \mathbf{X}_{r+n+t} + \varepsilon_{r+n+t} E^s_{\mathbf{X}_{r+n+t}}. \tag{1.13}$$

This equation can be solved by using the Newton-secant method.

We should emphasize that the values of m and t in Eq. (1.13) can be adequately adjusted for each system by an empirical procedure. Also, Hirsh and Pugh's theorem provides us with a proper way to use the approximation of the tangent subspace $E^s_{\mathbf{X}_i}$ and $E^u_{\mathbf{X}_i}$ at a point. According to that theorem, if we consider an orbit $\{\mathbf{X}_k\}_{k=1}^n$ which contains $\mathbf{X}_i$, any variation near $\mathbf{X}_{i-m}$ will expand

along the unstable manifold of $\mathbf{X}_i$ if m is chosen large enough. A similar statement can be made regarding the stable manifold of $\mathbf{X}_i$ for variations near $\mathbf{X}_{i+m}$ iterated in the backward direction.

That procedure can be used in the attempt to eliminate the recurrence in the original path from $\mathbf{p}_{\mathbf{X}_s}$ to $\mathbf{p}_{\mathbf{X}_t}$ that are less than δ_{lim}. Higher priority in the elimination should be assigned to the longest loops. A patch is accepted as usable if the perturbation ε_{r-m} to be applied, in order to implement it, is less than a preassigned limit value ε_{lim}. Our method spawns a sequence of perturbations $\{\varepsilon_i\}_{i=1}^{K}$ and directions $\{\boldsymbol{E}_i\}_{i=1}^{K}$ to be respectively applied to a sequence of points $\{\mathbf{X}_{n_i}\}_{i=1}^{K}$ of the original trajectory. To apply each perturbation, it is necessary to calculate the value $\widetilde{p_{\mathbf{X}_{n_i}}}$ of the parameter to be used in $\mathbf{X}_{n_i}$ to change the system state from $\mathbf{X}_{n_i}$ to $\mathbf{X}'_{n_i} = \mathbf{X}_{n_i} + \varepsilon_i \boldsymbol{E}_{x_i}$. The overall result of our method is a suboptimal constructive trajectory or a suboptimal pseudo-orbit that allows the transfer from $\mathbf{p}_{\mathbf{X}_s}$ to $\mathbf{p}_{\mathbf{X}_t}$.

The previous arguments can be consolidated in the following algorithm:

Step 1: Starting from the original transfer trajectory from $\mathbf{p}_{\mathbf{X}_s}$ to $\mathbf{p}_{\mathbf{X}_t}$, find all the recurrent points whose distance from it to its recurrent point is less than δ_{lim}. Sort them out by the size of the loop in decreasing order.

Step 2: Take from the list its first point and find a patch for the loop using Eq. (1.13). If the resulting perturbation is less than ε_{lim}, accept the patch. Put in the solution list the points in which the perturbation should be applied, together with the perturbations and the direction values.

Step 3: Take the next point in the list that is located after the previous found patch.

Step 4: Find a patch for the loop using Eq. (1.13). If the resulting perturbation is less than ε_{lim}, accept the patch. Put in the solution list the points in which the perturbation should be applied, together with the perturbations and the direction values.

Step 5: Go back to step 3 until all the points of the list have been considered.

Step 6: Use the solution list and the original trajectory to compute the pseudo-orbit that allows the suboptimal transfer from $\mathbf{p}_{\mathbf{X}_s}$ to $\mathbf{p}_{\mathbf{X}_t}$.

1.3.3 The Targeting Algorithm

The algorithm that results from the combination of parts I and II can be applied to general situations [31]. In fact, individually, each part has been successfully applied to numerical and laboratory experiments in mechanics [29, 46] and in situations involving spacecraft guidance [11]. Furthermore, with delay coordinate embedding, the algorithm is applicable to experimental situations in which no *a priori* analytical knowledge of the system dynamics is available [46].

The power of our method is due to the sequential combination of both parts. However, we must stress the fact that the second part has the objective of reducing the length of long trajectories that present recurrence to get a smaller trajectory. We can have situations where that algorithm does not succeed because

there is no recurrence in the trajectory for the specified limit values for the perturbation and the proximity between the recurrent points. In other situations, the trajectory found by the first part of the algorithm is short enough and already satisfies our goals.

1.4 Applying Control of Chaos and Targeting Ideas

In this section we apply the control of chaos concept in association with classical control methods. The proper combination of these two approaches gives rise to what we call the opportunistic chaos control strategy. We demonstrate this strategy by analyzing three very significative examples. In these examples, the chaotic invariant sets are nonattractive. In the first case, we consider a simple electronic circuit operating in a regime in which an attracting periodic orbit coexists with a chaotic saddle. As so, initial conditions not located on the periodic orbit generate trajectories that undergo a chaotic transient behavior until they eventually settle to the periodic orbit. In this system, a classic control steering method is used in association with the OGY to make the system behave periodically, and with a period that is different of the originally presented by the system after its transient interval.

In the second example, we analyze a very involved scenario with the presence of chaotic and no-chaotic behaviors that are entwined in state space in a very complicated way. Here our opportunistic chaos strategy combines the chaotic targeting approach and classic control methods to steer trajectories through the phase space and also to stabilize the system on periodic behaviors from time to time.

1.4.1 Controlling an Electronic Circuit

Let us consider an electronic circuit composed of an AC voltage source, a resistor, an inductor, and a diode as the nonlinear element, as shown in Fig. 1.1.

Applying the Kirchhoff voltage law, the voltage across the diode is related to the input voltage generator (V_{in}) and the circuit current by

$$L\frac{dI}{dt} = V_0 \sin(2\pi ft) - RI - V_d, \tag{1.14}$$

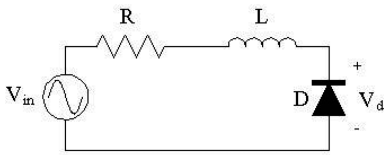

Fig. 1.1 Diode circuit: the diode circuit is composed of an AC voltage source V_{in}, a resistor R, an inductor L, and a diode; V_d is the voltage across the diode.

where V_0 is the voltage amplitude and f is the frequency.

For the diode, we consider its high-frequency model for the voltage across it, which is given by [19, 40]

$$V_d = \frac{|q|(C_j - C_d)}{2C_jC_d} + \frac{q(C_j + C_d)}{2C_jC_d} + E_0, \tag{1.15}$$

where q is the diode accumulated charge, C_j is the junction capacitance, and C_d is the diffusion capacitance.

Our system model equation can be converted to the following system of first-order autonomous differential equations:

$$\begin{cases} \dfrac{dq}{dt} = I \\ L\dfrac{dI}{dt} = V_0 \sin(\theta) - RI - \left(\dfrac{|q|(C_j - C_d)}{2C_jC_d} + \dfrac{q(C_j + C_d)}{2C_jC_d} + E_0 \right) \\ \dfrac{d\theta}{dt} = 2\pi f \end{cases} \tag{1.16}$$

For this work, we use the diode DIN1206C, which, according to the specifications, has for the parameters of its high-frequency model the values $453pF$ for the diffusion capacitance (C_d), 30 nF for the junction capacitance (C_j), and 0.52 V as the junction voltage (V_j). The circuit parameter values are $L = 0.18$ mH, and $R = 4.5\,\Omega$. For the input voltage generator, i.e., $V_{\text{in}} = V_o \sin(2\pi ft)$, we set $f = 333$ kHz, and V_0, the input voltage amplitude, is used as the variable parameter.

In Fig. 1.2, we show the system bifurcation diagram obtained by using a time-$2\pi f$ stroboscopic map.

Let us now look at the system dynamics inside the period-3 window. For this purpose and for $V_0 = 2.3$ V, we take a random initial condition located outside the period-3 window attractor and we obtain its trajectory. This trajectory, as it is observed in the previously defined time-$2\pi f$ stroboscopic map, appears in Fig. 1.3, while Fig. 1.4 shows the associated time series plot for the circuit current I. We can see that the system initially has a chaotic-like behavior. After this transient time, the trajectory finally settles on a period-3 periodic behavior. Further analysis indicated that this is a chaotic transient, which happens for this value of V_0 due to the presence of a nonattracting chaotic saddle that coexists with the period-3 attractor. Thus, trajectories starting from random initial conditions typically wander chaotically near this chaotic saddle for a finite time before settling down into the period-3 attractor. During the time interval in which the trajectory wanders chaotically, this trajectory presents in essence all the characteristics that are typical of a real chaotic trajectory. As so, during this time interval, it shows a sensitive dependence to changes in initial condition, as one of its finite-time Lyapunov exponents is greater than zero. Furthermore, embedded in the chaotic saddle, there are an infinite but numerable sets of unstable periodic orbits (UPO) of all periods.

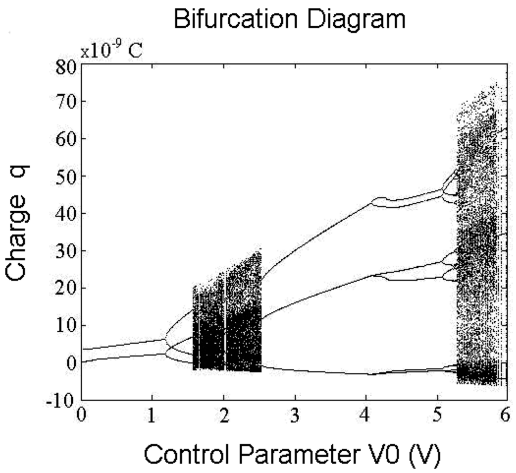

Fig. 1.2 Bifurcation diagram: diode circuit bifurcation diagram defined by a time-$2\pi f$ stroboscopic map; the time-$2\pi f$ mapped charge q against the control parameter V_0 varying from 0 to 5.8 V.

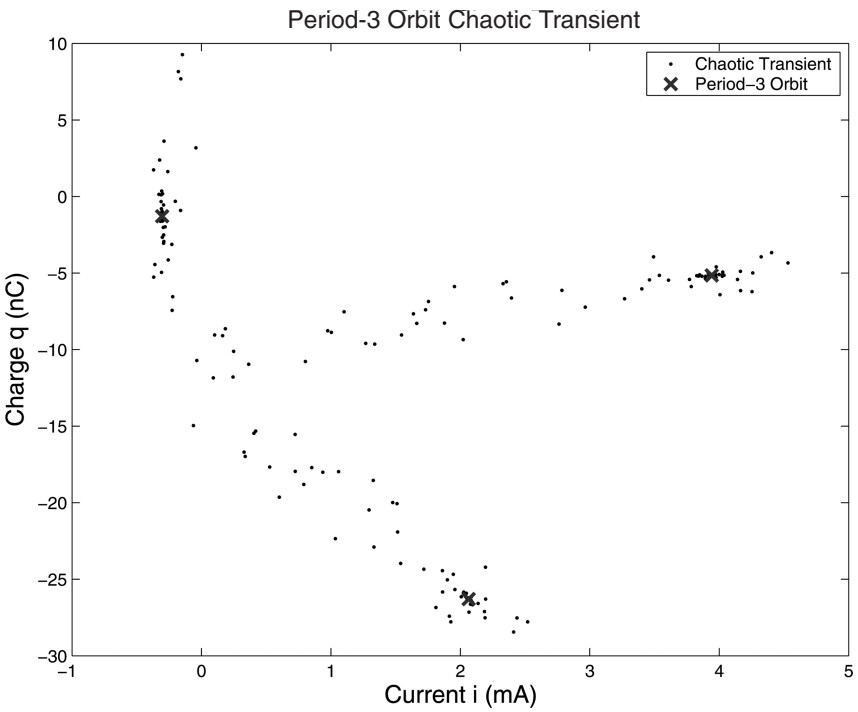

Fig. 1.3 Chaotic transient: chaotic transient before convergence to the period-3 orbit at $V_0 = 3.8$ V and $f = 333$ kHz.

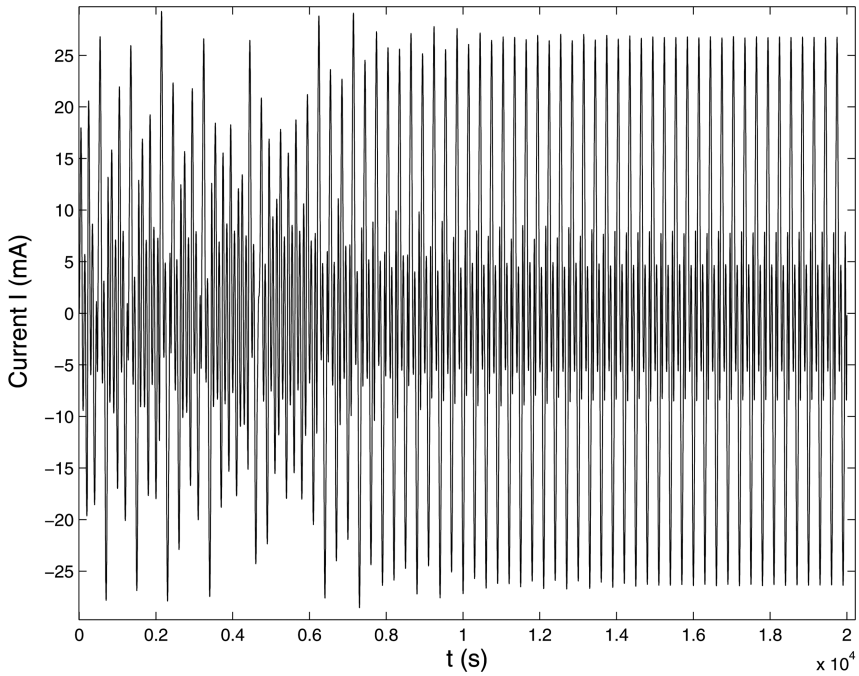

Fig. 1.4 Chaotic transient time series: Current I (mA) versus time transient before convergence to the period-3 orbit at $V_0 = 3.8$ V and $f = 333$ kHz.

Let us now assume that we want to stabilize the system in one of these *UPO*. The original OGY method depends on ergodicity to bring a chaotic trajectory sufficiently close to the desired *UPO* so to stabilize the system. However, we are now dealing with a system in which the behavior is not chaotic, but it is a chaotic transient. As so, a typical trajectory might not pass close to the desired unstable periodic orbit embedded in the chaotic saddle. To overcome this difficulty related to accessibility of the unstable periodic orbits by a chaotic transient trajectory, we use our opportunistic chaos control strategy: a classical nonlinear control method is strategically associated with the *OGY* chaos control strategy. The classical method is used first, just to drive the trajectory to the neighborhood of the *UPO*. From these point on, the *OGY* strategy is then applied so that the system is kept stabilized by using small perturbations.

This classical nonlinear control method, called *input–output linearization* [47], works as follows: consider a guiding control problem and a nonlinear system,

$$\dot{\mathbf{x}} = \mathbf{f}(\mathbf{x}, u) \qquad (1.17)$$
$$, y = h(\mathbf{x}),$$

where u is the control parameter.

Assume that our goal is to make the output $y(t)$ follows the desired output $y_d(t)$, where $y_d(t)$ is well known and limited (not diverging). Note that the output $y(t)$ is not directly related to the control parameter u. Consequently, in general, it is not easy to find out how the input u should be designed to control and guide the output $y(t)$. However, in many situations it is possible to find out a simple and direct functional relationship between the output $y(t)$ and the control parameter u.

In our system model, represented by Eq. (1.16), let us redefine its variable as follows: $q = x_1$, $I = x_2$, $y = x_1$, $\theta = x_3$, and $V_0 = u$, so that the system is now described by the following equations:

$$\begin{cases} \dfrac{dx_1}{dt} = x_2 \\ L\dfrac{dx_2}{dt} = u\sin(x_3) - Rx_2 - \left(\dfrac{|x_1|(C_2 - C_1)}{2C_2C_1} + \dfrac{x_1(C_2 + C_1)}{2C_2C_1} + E_0\right) \\ \dfrac{dx_3}{dt} = 2\pi f \\ y = x_1 \end{cases} \tag{1.18}$$

To find a functional relation between the output y and the input u, we differentiate the output y twice

$$\ddot{y} = ((1/L)\sin(x_3))u + f_1(\mathbf{x}), \tag{1.19}$$

where $f_1(x)$ is a state function defined by

$$f_1(\mathbf{x}) = (1/L)\left(- Rx_2 - \left(\frac{|x_1|(C_2 - C_1)}{2C_2C_1} + \frac{x_1(C_2 + C_1)}{2C_2C_1} + E_0\right)\right). \tag{1.20}$$

Equation (1.19) is a direct relation between the output y and the input u. Now, if we choose the input control as follows

$$u = \frac{L}{\sin(x_3)}(v - f_1), \tag{1.21}$$

where v is the new input to be determined, the nonlinearity presented in Eq. (1.19) is canceled and we get a linear relationship between the output and the new input v:

$$\ddot{y} = v. \tag{1.22}$$

Let us make $e = y(t) - y_d(t)$ the guiding error. We choose the new input control as follows:

$$v = \ddot{y}_d - k_1 e - k_2 \dot{e}, \tag{1.23}$$

where k_1 and k_2 are positive constants.

From Eqs. (1.22) and (1.23), we get the closed loop guiding error differential equation

$$\ddot{e} + k_1 e + k_2 \dot{e} = 0. \tag{1.24}$$

This equation can be transformed to its characteristic form

$$\lambda^2 + k_1 \lambda + k_2 = 0 = (\lambda - p_1)(\lambda - p_2). \tag{1.25}$$

As so, it is possible to choose the appropriates constants k_1 and k_2 to properly allocate the poles of the linearized system. Thus, at each iteration the constants k_1 and k_2 are properly chosen and the new input value is estimated in accordance with the desired output $y_d(t)$ and the current error $e(t)$.

In Fig. 1.5, we show the results of applying our opportunistic chaos control method for this system in an extreme situation. The system is initially on the period-3 periodic orbit. Our method is successively used to stabilize the system on unstable periodic orbits of periods 1, 2, 4, and 8.

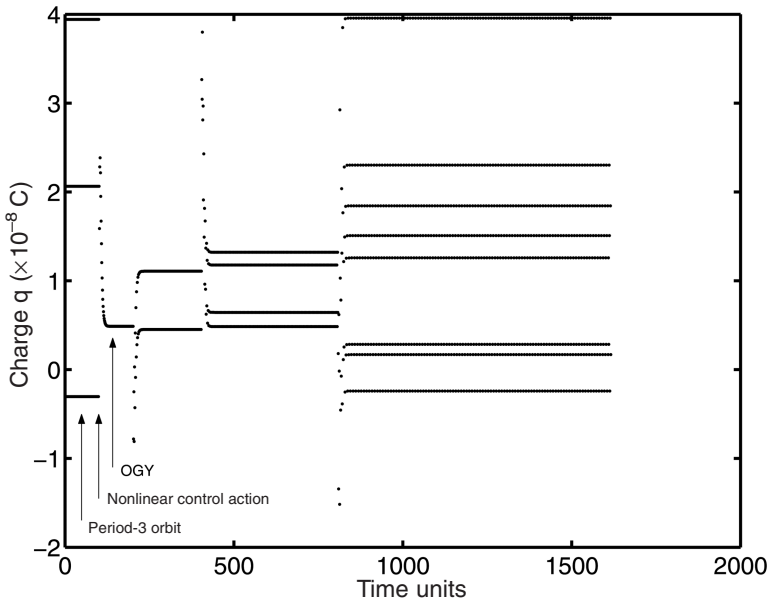

Fig. 1.5 Control in chaotic saddles: the figure shows the system period-3 regime followed by a transient classic control that conducts the orbit to an ε-neighborhood of the desired fixed point (periodic point) when the OGY control is applied.

1.4.2
Controlling a Complex System

To construct a complex dynamical system, let us consider the kicked single rotor, which describes the time evolution of a mechanical pendulum that is being kicked at times $nT, n = 1, 2, \ldots$, with a constant force f_0. From the differential equation for this mechanical system one can derive a Poincaré map which is related to the state of the system just after each successive kick [43]:

$$\begin{aligned} x_{k+1} &= x_k + y_k (mod 2\pi) \\ y_{k+1} &= (1 - v) * y_k + f_0 \sin(x_k + y_k), \end{aligned} \tag{1.26}$$

where x corresponds to the phase and y to the angular velocity. f_0 is the force parameter, and v is the damping parameter, measuring the energy dissipation of the system. The parameter v varies between 0, for a Hamiltonian situation, with no damping, and 1, in the case of a very strong damping. The dynamics lies on the cylinder $[0, 2\pi) \times \Re$.

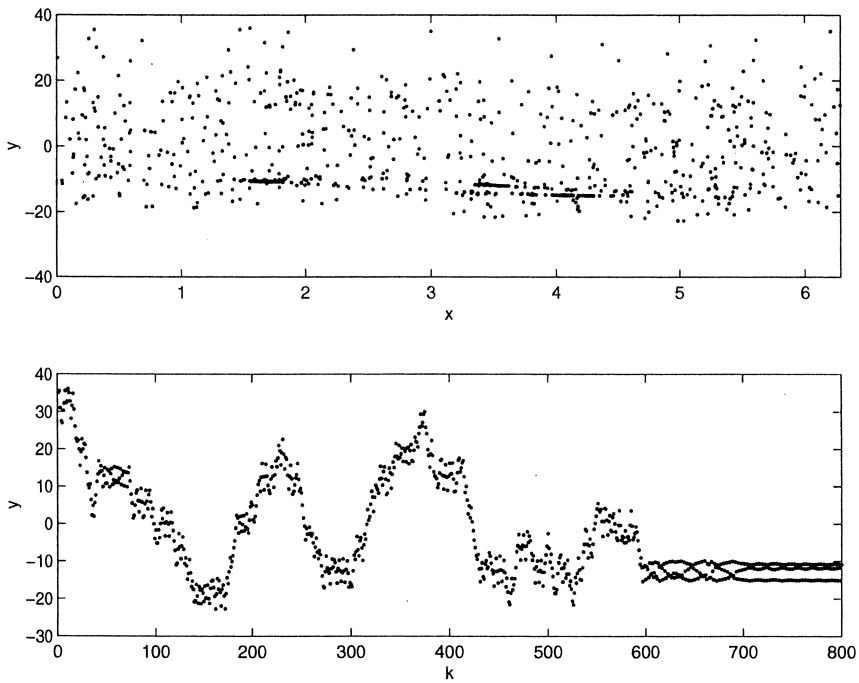

Fig. 1.6 Typical trajectory of the kicked single rotor with the parameters $f_0 = 4.0$ and $v = 0.02$. The y variable represents the angular velocity, x represents the phase, and k represents the iteration number. In both graphs, all plotted quantities are dimensionless.

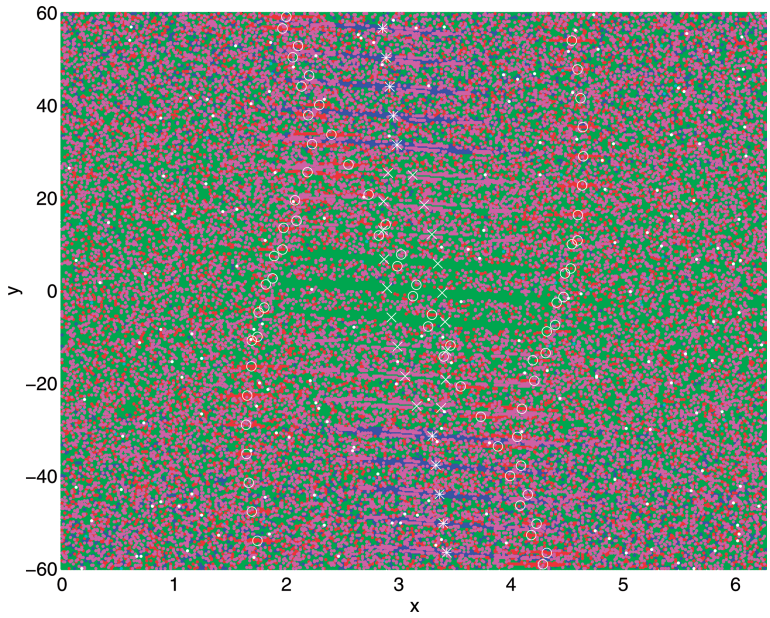

Fig. 1.7 Basin of attraction for the kicked single rotor. The colors identify the periodicity of the orbits, while the characters identify the location of the attracting periodic orbits. In the figure, "*" indicates the position of attracting period one points, "x" the position of attracting period two orbits, and "o" the position of attracting period three orbits. This picture is for the following parameters: $f_0 = 4.0$ and $\nu = 0.02$. All quantities plotted are dimensionless.

In the Hamiltonian case (no damping, $\nu = 0$), we have the area-preserving standard map, which was studied by Chirikov [12] and by many other authors [36, 42]. It has stable and unstable periodic orbits, Kolmogorov-Arnol'd-Moser (KAM) surfaces, and chaotic regions. Depending on the nonlinear parameter f_0, the regions of regular motion and the regions of chaotic motion are complexly interwoven. As the second equation of the map is also taken to be modulo 2π, the map of the cylinder reduces now to the map of the torus $[0, 2\pi) \times [0, 2\pi)$ to itself. As a consequence, each of the periodic orbits represents, in fact, a family of overlapping periodic orbits in which the velocity y differs by integer multiples of 2π. Because of the modulo 2π, all periodic orbits of the same family are located at the same location on the torus.

If we now consider the Hamiltonian case but introduce a very small amount of dissipation (ν value close to zero), the motion again takes place on the cylinder $[0, 2\pi) \times \Re$ in order to preserve the invariant structure. The periodic orbits become sinks and the chaotic Hamiltonian sets become saddle chaotic invariant sets embedded in the basin boundaries separating the various sinks. The chaotic motion is hence replaced by long chaotic transients that occur before the trajectory is eventually asymptotic to one of the sinks [16], as can be seen in a typi-

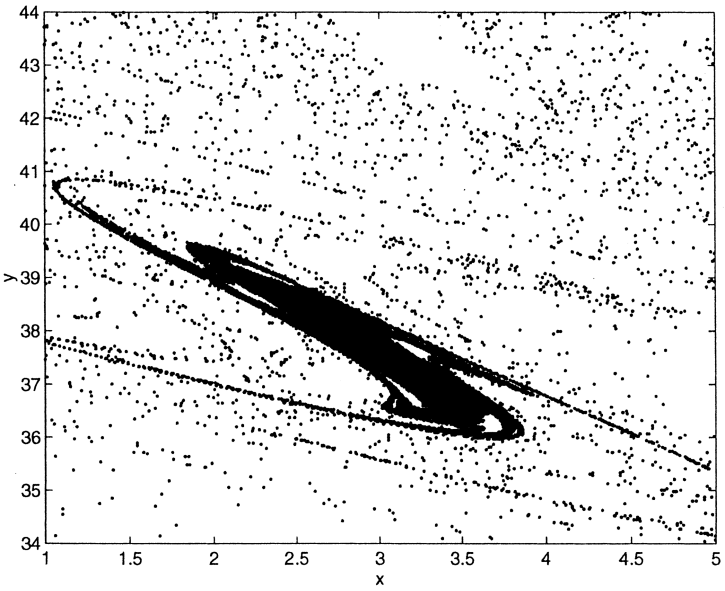

Fig. 1.8 Enlargement of the basin of attraction for a period-1 attracting orbit. Points located inside the region $[1.0, 5.0] \times [34.0, 44.0]$ that go to this period-1 attracting orbit are plotted. All quantities plotted are dimensionless.

cal trajectory that appears in Fig. 1.6. Furthermore, the dissipation leads to a separation of the overlapping periodic orbits, which belong to a given family, with increasing modulo of the velocities on the cylinder. However, there is a bounded cylinder which contains all of the attractors [16]. This cylinder is given as $[0, 2\pi) \times [-\gamma_{\max}, \gamma_{\max}]$, where $\gamma_{\max} = f_0/\nu$, and all trajectories are eventually trapped inside this region [16]. Consequently, for values of ν close to zero, there is a large, but finite, number of coexisting periodic orbits of increasing period. Figure 1.7 is a picture in the space of initial conditions showing the basins of attraction for all attractors of periods 1 to 3. The periodicity of the attractors in the picture is distinguished by gray scales, while the locations of the attracting periodic orbits are identified by special characters that are mentioned in the figure caption.

Figure 1.8 shows a typical basin of attraction for the period-1 attracting orbit at $y = 6\pi$. The black points are attracted to this attractor. The basins of attraction have fractal boundaries, with the box counting dimension d of the basin boundary equal to $d = 1.999$. This means that the dimensions of the basin boundaries is nearly the dimensions of the state space, and they are organized in a complexly interwoven structure, with chaotic saddles embedded in these basin boundaries [23]. Furthermore, extremely small changes in the initial conditions may shift a trajectory from one basin to another, which means that the system has high sensitivity to the final state. Thus, which attractor is eventually

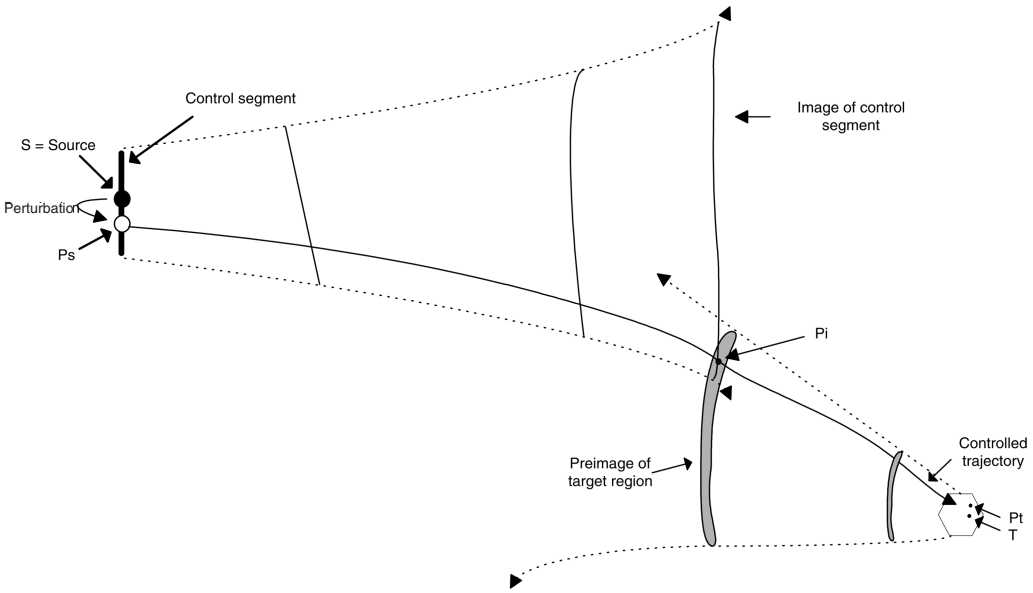

Fig. 1.9 Schematic representation of the scenario involving the use of part I of our targeting procedure for a two-dimensional system.

reached by a trajectory of the system depends strongly on the initial conditions. In this scenario, typical trajectories, starting with arbitrary initial conditions, experience periods of long chaotic transients due to the saddle chaotic invariant sets, before approaching one of the periodic attractors.

Let us consider two points x_s and x_t, both of which located in the neighborhood of the fractal basin boundary. Our objective is to apply our targeting procedure to find a pseudo-orbit that goes from a point $p_{x_s} \in B_\varepsilon(x_s)$ to a point $p_{x_t} \in B_\varepsilon(x_t)$, where ε is a specified small value. The scenario involving the use of part I, as described in Section 1.3, of the targeting algorithm is depicted in Fig. 1.9. In this case, the dimension of the space is 2. To apply part I of the targeting algorithm, we uniformly distribute random points in the interior of the circle $B_\varepsilon(x_s)$. In this case, the result of a Delaunay triangulation is a polygon, which is iterated backward, while the "control segment" is iterated forward. The result of this procedure can be seen in Fig. 1.10. For this particular situation, part I of the algorithm is able to find a trajectory that takes just 30 iterations to reach $p_{x_t} \in B_\varepsilon(x_t)$. We consider this result good enough and decide that it is not necessary to apply part II of the algorithm. It is important to reaffirm that for low dimension systems, in general, just part I produces a good result.

The procedure just described works for points located in the neighborhood of the fractal basin boundaries. It works because of the inherent exponential sensitivity of the chaotic time evolution to perturbations. Therefore, the source point x_s and the targeting point x_t *must* both be in the same neighborhood of the

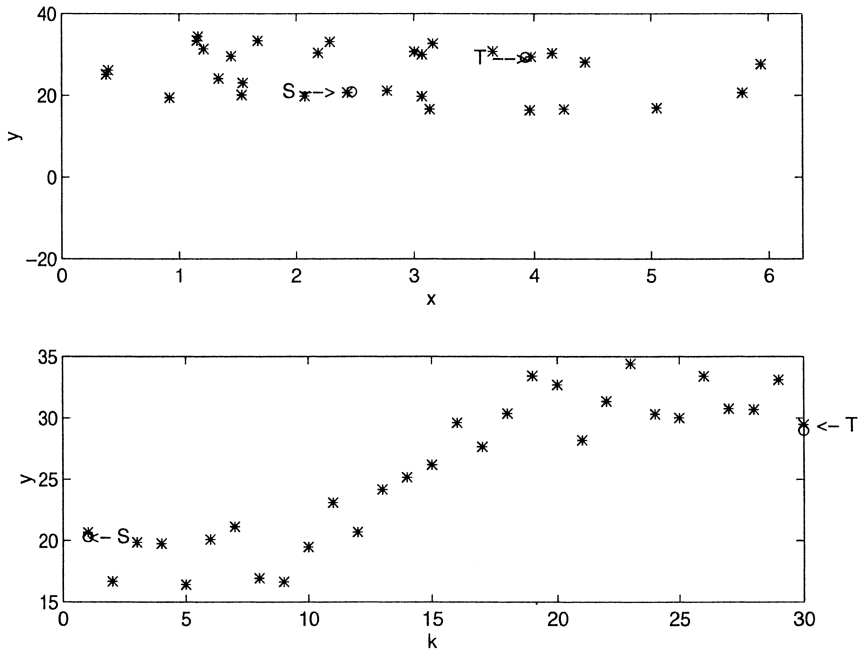

Fig. 1.10 By exploring the chaotic behavior of the system, our targeting procedure rapidly steers the trajectory from *S* to *T*. The asterisks represent the trajectory obtained by applying our targeting procedure to drive the system from the point *S* to the point *T*. The *y* variable represents the angular velocity, *x* represents the phase, and *k* represents the iteration number. In both graphs, all quantities plotted are dimensionless.

chaotic invariant set. This is the case for the points x_s and x_t of the previous example. However, if the system is evolving in a regular regime (not chaotic), the condition of being located in the same chaotic invariant set is not satisfied. Furthermore, the time evolution is "ordered," and the inherent exponential sensitivity to perturbations does not apply. However, we show next that if the objective is to bring the trajectory from one stable state to another stable state, we can first guide the trajectory to the basin boundary structure, where the chaotic saddles are located, and there apply our targeting method. Thus, the idea, which is illustrated in Fig. 1.11, is as follows: (i) remove the trajectory from the basin of attraction of the initial stable periodic orbit, (ii) apply the targeting procedure in the basin boundary to bring the trajectory to the neighborhood of the basin of attraction of the desired stable periodic orbit and finally (iii) bring the trajectory to the desired stable periodic orbit. We can accomplish this guidance task inside the basin of attraction of the stable periodic orbits (i) and (iii) by using a classical technique from the system control theory and outside the basins of attraction (in the chaotic invariant region) (ii) using the targeting procedure just described. This approach stresses the powerful tool that we developed by combining classical control techniques with chaos control methods.

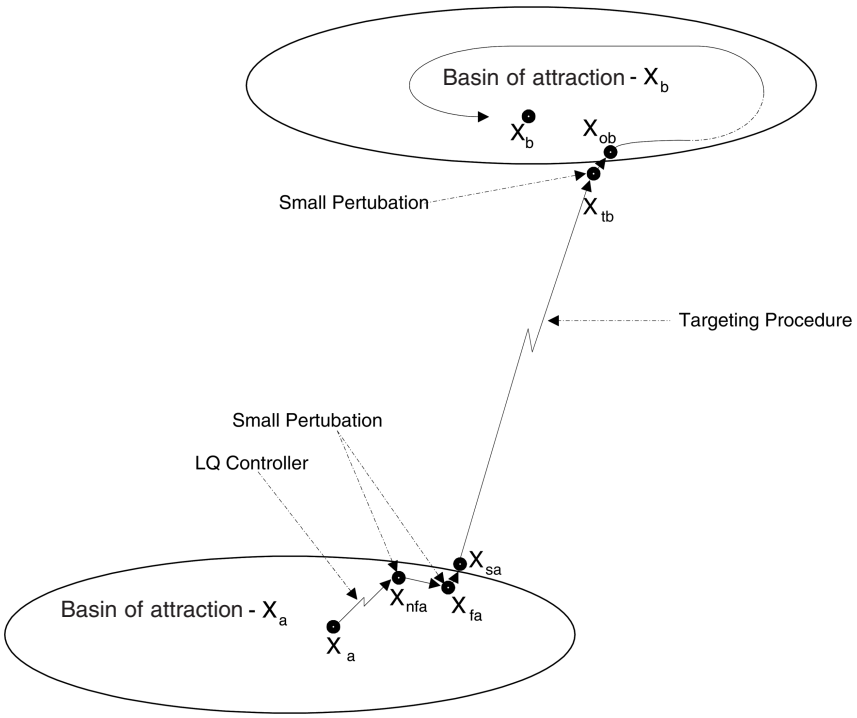

Fig. 1.11 Schematic representation of our complete targeting procedure. The system was evolving in a periodic orbit X_a. Our goal is to steer it to another periodic orbit X_b. The *LQ controller* drives the trajectory from X_a to a point X_{nfa} near X_{fa}. In X_{nfa} a small perturbation is applied, and the system moves to the state X_{fa}. Another perturbation is applied, and the system moves to the state X_{fa}. Our chaotic targeting procedure is then used to stir the system to X_{tb}. Another small perturbation drives the system to the point X_{ob}, that belongs to the basin of attraction of X_b. From this point, the system's natural dynamics drives the trajectory to the desired stable periodic orbit X_b.

To accomplish (i), we can use, for example, a classical optimal control method, such as the *LQ controller* [3]. As the basin of attraction of the stable periodic orbits is small open regions around the periodic orbits, it is possible to linearize the system about the points $\{x_i\}_{i=1}^{n_p}$ of the orbit, which gives

$$z_{k+1} = A(x_i)z_k, \tag{1.27}$$

where $A(x_i)$ is $Df(x_i)$. To change the state of the system, it is necessary to introduce an input term to Eq. (1.27) as

$$z_{k+1} = Az_k + Bu_k, \tag{1.28}$$

where u_k is the vector of inputs and B is a constant matrix that states how the inputs influence the state of the system. The objective is to pick u_k so that the "cost function"

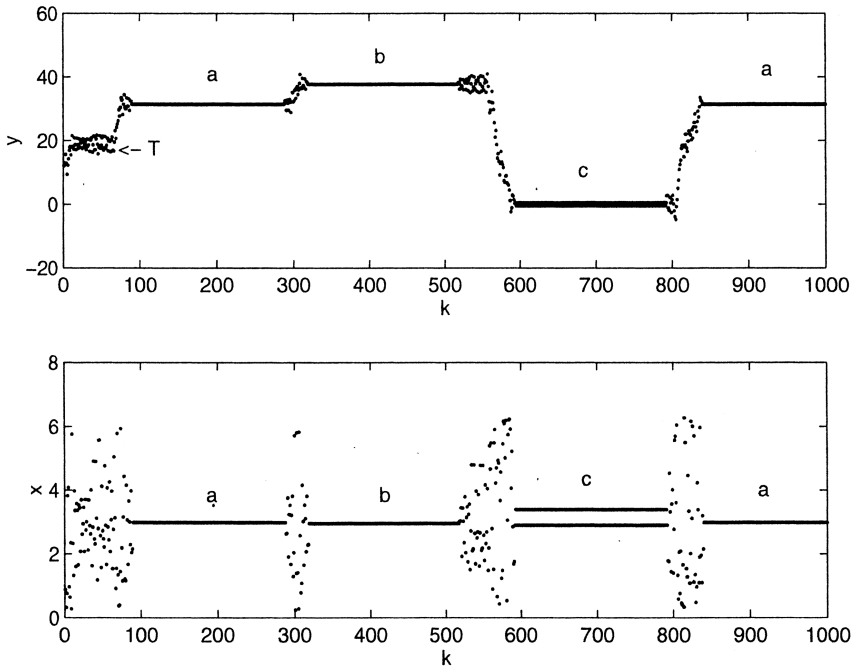

Fig. 1.12 Results of applying our combined method of control to change the system evolution among stable periodic orbits. The *y* variable represents the angular velocity, *x* represents the phase, and *k* represents the iteration number. In both graphs, all quantities plotted are dimensionless.

$$J = 1/2 \sum_{k=0,N} (z_k^t Q_1 z_k + u_k^t Q_2 u_k) \tag{1.29}$$

is minimized. Q_1 and Q_2 are symmetric and positive definite weighting matrices to be selected based on the relative importance of the various states and controls. The well-known solution technique can now be applied (see [3]).

As our targeting procedure, applied in (ii), is able to drive the trajectory to the neighborhood of the basin of attraction of the desired stable periodic orbit, just a small perturbation can be used to send the orbit from that point to the interior of the basin of attraction. Once there, the system dynamics is enough to drive the trajectory to the desired stable periodic orbit. Thus, (iii) can be easily accomplished. However, another control system technique could be applied, if desired.

In Fig. 1.12 we show the results of applying that combined method to change the system evolution among the desired stable periodic orbits. When our targeting method is applied, the perturbations that are necessary to create the pseu-

do-orbit and send the orbits to the interior of the basin of attraction of the stable periodic orbits are less than 0.1.

1.5 Conclusion

In 1990, the concept of controlling chaos came about showing that not only the chaotic evolution could be controlled, but also the complexity inherent on the chaotic dynamics could be exploited to provide a unique level of flexibility and efficiency in technological uses of chaotic systems. Over the years, we have witnessed a variety of applications for this concept in almost all areas of knowledge. In parallel, new methods appear, each one tailored to specific situations or trying to improve previously released control of chaos methods. Despite this tremendous development and research, the fundamental ideas embedded in this concept must be kept in focus. With this chapter, we envisage not only the assessment of those fundamental ideas but also to point out paths to be followed in future development. As so, we summarize it with the following:

- Controlling of chaos is based on small perturbations applied to sensitive systems in order to opportunistically exploit its dynamics. It is based on the flexibility that such a system can provide. Feedback strategies may be used, but just locally to a particular trajectory.
- Controlling of chaos can be applied wherever chaos is present. This means that its application is not only restricted to attracting sets, but can also be used in nonattracting ones, situations in which we can produce interesting results.
- Control of chaos strategies can be combined with classic control strategies to convey powerful, opportunistic, and efficient control mechanisms that exploit the limits of flexibility that the system can provide.

References

1 F. T. Arecchi, R. Meucci, G. Puccioni, and J. Tredicce. Experimental evidence of subharmonic bifurcations, multistability, and turbulence in a q-switched gas laser. *Phys. Rev. Lett.,* 49:1217–1220, 1982.

2 D. K. Arrowsmith and C. M. Place. *An Introduction to Dynamical Systems.* Cambridge University Press, 1990.

3 K. J. Aström and B. Wittenmark. *Computer Controlled System: Theory and Design.* Prentice-Hall, Englewood Cliffs, NJ, 1984.

4 A. Azevedo and S. M. Rezende. Controlling chaos in spin-wave instabilities. *Phys. Rev. Lett.,* 66:1342–1345, 1991.

5 G. L. Baker. Control of the chaotic driven pendulum. *Am. J. Phys.,* 63(9):832–838, 1995.

6 E. Barreto, E. J. Kostelich, C. Grebogi, E. Ott, and J. A. Yorke. Efficient switching between controlled unstable orbits in higher dimensional chaotic systems. *Phys. Rev. E,* 51:4169–4172, 1995.

7 E. Belbruno, *Capture and Chaotic Motions in Celestial Mechanics: with Applications to the Construction of Low Energy Transfer.* Princeton University Press, 2004.

8 S. Bielawski, D. Derozier, and P. Glorieux. Controlling unstable periodic orbits by a delayed continuous feedback. *Phys. Rev. E,* 49:971–974, 1994.

9 S. Bleher, C. Grebogi, and E. Ott. Bifurcation to chaotic scattering. *Physica D,* 46:87–121, 1990.

10 E. M. Bollt and J. D. Meiss. Controlling chaotic transport through recurrence. *Physica D,* 81:280–294, 1995.

11 E. M. Bollt and J. D. Meiss. Targeting chaotic orbits to the moon through recurrence. *Phys. Rev. A,* 204:373–378, 1995.

12 B. V. Chirikov. A universal instability of many-dimensional oscillator systems. *Phys. Rep.,* 52:265–379, 1979.

13 D. L. DeAngelis, W. M. Post, and C. C. Travis. *Positive Feedback in Natural Systems*. Springer, Berlin, 1986.

14 R. Devaney. *An Introduction to Chaotic Dynamical Systems*. Persus Books, Cambridge, MA, 1989.

15 W. L. Ditto, S. N. Tauseo, and M. L. Spano. Experimental control of chaos. *Phys. Rev. Lett.,* 65:3211–3214, 1990.

16 U. Feudel, C. Grebogi, B. Hunt, and J. A. Yorke. Map with more than 100 coexisting low-periodic attractors. *Phys. Rev. E,* 54:71–81, 1996.

17 A. Garfinkel, M. L. Spano, W. L. Ditto, and J. N. Weiss.Controlling cardiac chaos. *Science,* 257:1230–1233, 1992.

18 J. L. Gouze. Positive and negative circuits in dynamical systems. *J. Biol. Systems,* 6:11–15, 1998.

19 P. E. Gray and C. L. Searle. *Princípios de Eletrônica*. Livros Técnicos and Científicos Ed. S.A, 1977.

20 C. Grebogi, E. Kostelich, E. Ott, and J. A. Yorke. Multi-dimensioned interwined basin boundaries: Basin structure of the kicked double rotor. *Physica D,* 25:347–360, 1987.

21 C. Grebogi and Lai. Controlling chaotic dynamical systems. *Syst. Control Lett.,* 31:307–312, 1997.

22 C. Grebogi, Y. C. Lai, and S. Hayes. Control and applications of chaos. *J. Franklin Inst.,* 334B:1115–1146, 1997.

23 C. Grebogi, E. H. Nusse, E. Ott, and J. A. Yorke. Basic sets: Sets that determine the dimensions of basin boundaries. In J. C. Alexander, editor, *Lecture Notes in Mathematics,* vol. 1342, pp. 220–250. Springer, Berlin, 1988.

24 C. Grebogi, E. Ott, and J. A. Yorke. Crises, sudden changes in chaotic attractors, and transient chaos. *Physica D,* 7:181–200, 1983.

25 J. Guckenheimer and P. Holmes. *Nonlinear Oscilations, Dynamical Systems, and Bifurcations of Vector Fields*. Springer, Berlin, 1983.

26 S. Hayes, C. Grebogi, and E. Ott. Communicating with chaos. *Phys. Rev. Lett.,* 70:3031, 1993.

27 G. H. Hsu, E. Ott, and C. Grebogi. Strange saddles and the dimensions of their invariant manifold. *Phys. Lett. A,* 127(4):199–204, 1988.

28 H. Kantz and P. Grassberger. Repellers, semi-attractors, and long-lived chaotic transients. *Physica D,* 17:75–86, 1985.

29 E. J. Kostelich, C. Grebogi, E. Ott, and J. A. Yorke. Higher-dimensional targeting. *Phys. Rev. E,* 47:305–310, 1995.

30 E. E. N. Macau. Targeting in chaotic scattering. *Phys. Rev. E,* 57:5337–5346, 1998.

31 E. E. N. Macau and C. Grebogi. Driving trajectories in complex systems. *Phys. Rev. E,* 59:4062–4069, 1999.

32 E. E. N. Macau. Using chaos to guide a spacecraft to the moon. *Acta Astronautica,* 47:871–878, 2000.

33 E. E. N. Macau. Exploiting unstable periodic orbits of a chaotic invariant set for spacecraft control. *Celes. Mech. Dyn. Sys.,* 87:291–305, 2003.

34 E. E. N. Macau and C. Grebogi. Driving trajectories in chaotic systems. *Int. J. Bifurcat. Chaos,* 11:1423–1442, 2001.

35 K. S. McCann. The diversity-stability debate. *Nature,* 405:228–233, 2000.

36 J. D. Meiss, J. R. Lary, J. D. Crawford, C. Grebogi, A. N. Kaufway, and H. D. I. Abrabanel. Correlations of periodic, area-preserving maps. *Physica D,* 6:375–384, 1983.

37 R. Meucci, W. Gadomski, M. Ciofini, and F. T. Arecchi. Experimental control of chaos by means of weak parametric perturbations. *Phys. Rev. E,* 49:2528–2531, 1994.

38 E. Ott, C. Grebogi, and J. A. Yorke. Controlling chaotic dynamical systems. In D. Campbell, editor, *CHAOS/XAOC, Soviet-Amer. Perspective on Nonlinear Science,* pp. 153–172. Amer. Inst. Phys., 1990.

39 E. Ott, C. Grebogi, and J.A. Yorke. Controlling chaos. *Phys. Rev. Letts.*, 64(11): 1196–1199, 1990.

40 J.F. Pierce. *Dispositivos de Junção Semicondutores.* Ed. USP, 1972.

41 S.J. Schiff, K. Jerger, D.H. Duong, T. Chang, M.L. Spano, and W.L. Ditto. Controlling chaos in brain. *Nature*, 370:615–620, 1994.

42 G. Schmidt. Stochasticity and fixed-point transitions. *Phys. Rev. A*, 22:2849–2854.

43 G. Schmidt and B.W. Wang. Dissipative standard map. *Phys. Rev. A*, 32:2994–2999, 1985.

44 T. Shinbrot, W. Ditto, C. Grebogi, E. Ott, M. Spano, and J.A. Yorke. Using the sensitive dependence of chaos (the "butterfly effect") to direct trajectories in an experimental chaotic system. *Phys. Rev. Lett.*, 68:2863–2866, 1992.

45 T. Shinbrot, E. Ott, C. Grebogi, and J.A. Yorke. Using chaos to direct trajectories to targets. *Phys. Rev. Lett.*, 65:3215–3218, 1990.

46 T. Shinbrot, E. Ott, C. Grebogi, and J.A. Yorke. Using chaos to direct orbits to targets in systems describable by a one-dimensional map. *Phys. Rev. A*, 45:4165–4168, 1992.

47 E. Slotine and W. Li. *Applied Nonlinear Control.* Prentice-Hall, Englewood Cliffs, NJ, 1991.

48 S. Smale. Differentiable dynamical systems. *Bull. Amer. Math. Soc.*, 73:747–817, 1967.

49 R. Thomas and R. D'Ari. *Biological Feedback.* CRC Press, Boca Raton, FL, 1990.